Density functional calculations as a tool for the characterization of ultrahin organic films: synthesis and spectroscopic characterization of RDX "monolayers" on glass substrates

Perla Torres*, Ismael Cotte*, Nairmen. Mina*, Samuel P. Hernandez*, R.T. Chamberlain**, Jorge Garcia***, Richard Lareau** and Miguel E. Castro*

* Department of Chemistry, The University of Puerto Rico at Mayaguez, Mayaguez, Puerto Rico 00682; miguel_castro99@hotmail.com

** Visiting scholar, permanent address: Federal Aviation Administration, William J. Hughes Technical Center, Atlantic City, New Jersey, 08405.

*** Hewlett Packard Imaging and Printing Supplies Operations Puerto Rico, Technical Services Group, Aguadilla, Puerto Rico, 00605.

ABSTRACT

Density functional theory calculations (DFT), Raman and atomic force microscopy (AFM) were employed to study the surface chemistry of ultra thin films of RDX on glass substrates. The preparation method played a major role in the morphology of the RDX films. Dispersed particles (500 nm) and larger (25 μm) crystals were observed in AFM. The vibrational fingerprint of RDX indicates the presence of β and α RDX phases. DFT calculations predict the RDX molecule to have all three NO_2 groups in axial position with respect to a distorted triazine ring. The agreement between calculated and measured Raman frequencies was excellent. Measured Raman intensities and depolarization ratios were found to lie between 0.61 and 0.75, indicating that the vibrational modes have low symmetry.

INTRODUCTION

Hexahydro-1,3,5-trinitro-s-triazine, better known as RDX, is a powerful secondary explosive that has attracted considerable attention due to its interesting structure and unique properties[1]. The structure of gas phase RDX obtained from density functional theory calculations at the 6-311++G** level is shown in scheme I. It consists of three NO_2 groups bonded to the nitrogen atoms of the chair conformer of a triazine ring. In the solid state, two RDX structures are known. These two structures differ by the spatial orientation of the NO_2 groups with respect to the triazine ring. In β RDX, all NO_2 groups are believed to be oriented in axial position. In α RDX one NO_2 group is located in equatorial and two NO_2 groups are in axial positions with respect to the triazine ring. We report here results on the synthesis and characterization of β RDX on glass and aluminum substrates using Raman, atomic force microscopy and X-ray photoelectron spectroscopy (XPS). Raman microscopy is a very attractive approach for a selective sensor development due to its sensitivity to phase symmetry. Interpretation of Raman data, however, requires detailed knowledge of the structure and vibrational modes of the phases examined. We have expanded earlier theoretical work by performing calculations at the B3LYP level using the 6-311++G**

Scheme I: Optimized RDX structure at the DFT/6-311++G** level.

basis set to determine Raman frequencies, intensities, and depolarization ratios. We found a close agreement between measured and calculated vibrational frequencies for β and gas phase RDX, respectively. The agreement between measured and calculated Raman intensities and depolarization was very poor. We found no evidence for strongly polarized Raman bands, which suggests that the RDX molecules in the β phase do not have strongly symmetric vibrational modes or may consists of randomly oriented molecules.

EXPERIMENTAL

Raman spectra were acquired using a commercial Renishaw RM 2000 Raman Microspectrometer with vibrational and white light imaging capabilities. The

514.5 nm line of a Coherent INNOVA 308 Ar^+ ion laser was used as the excitation source for the Raman measurements. RDX was deposited on the substrates from a RDX/acetonitrile solution purchased from Cerilliant. The solvent was allowed to evaporate at room temperature after the deposition. No signals due to acetonitrile where observed in the Raman measurements reported here. Raman intensities reported here have been corrected for detector sensitivity, determined by comparing the Raman spectrum of aspirin with literature values. Density functional theory calculations (DFT) were performed using the Gaussian 98 (GAUSSIAN, Inc., Pittsburgh, PA) package in a Dell Dimension XPS T450 desktop computer system. The Hyperchem software package was used for visualization purposes. AFM measurements were performed in a Parks instrument.

RESULTS

Representative AFM images following RDX deposition on a roughened aluminum substrate is shown on figure 1. Small particles, of about 500 nm in size, are readily identified on figure 1.

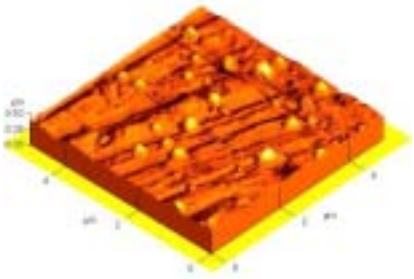

Figure 1: AFM measurements of β RDX particles on a rough aluminum substrate.

Single particle Raman spectroscopy measurements revealed that the ring breathing frequency in these particles is centered at about 877 cm^{-1}, consistent with the presence of the β RDX phase. Clean patches of the aluminum substrate are clearly distinguishable from RDX covered areas, indicating that amount of RDX deposited is not enough to saturate the substrate surface. Homogenous deposition of larger amounts of RDX resulted in the formation of RDX layers with a vibrational fingerprint characteristic of α RDX. AFM images on glass substrates showed the formation of islands of β RDX particles.

The lower trace in figure 2 shows the Raman spectrum between 100 and 1750 cm^{-1} (left panel) and between 2850 and 3150 cm^{-1} (right panel) obtained for the glass substrate used in the work presented here. Only broad signals at 1113.5 and 581.9 cm^{-1} are observed in Raman measurements of the glass substrate. The middle and upper traces in figure 2 represent typical Raman spectra obtained following the exposure of a glass substrate to the RDX/acetonitrile aerosol for enough time to form the β and α RDX phases, respectively. The glass substrate signals were readily attenuated after the deposition of β RDX particles on the substrate.

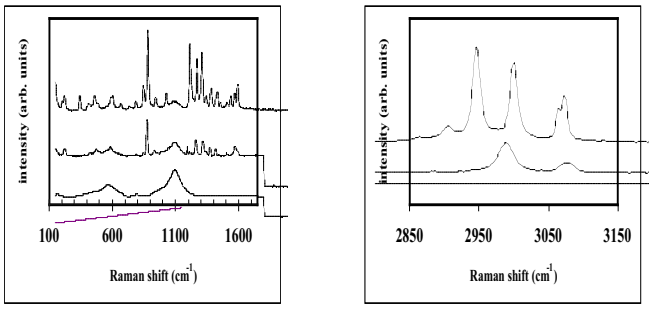

Figure 2: The lower, middle and upper traces represent the Raman spectra of the glass substrate, the β and α RDX phases, respectively. The left and right panels represent the Raman spectra between 100 and 1750 cm^{-1} and between 2850 and 3150 cm^{-1}, respectively.

The Raman spectra of β RDX is characterized by an intense signal at about 877 cm^{-1} due to the symmetric ring breathing mode. Weaker signals are observed below the symmetric ring-breathing mode. These signals are centered at 600, 498 and 234 cm^{-1} due to the NO_2 scissors and rocking modes, respectively. A number of methylene deformations and symmetric NO_2 stretches are observed between 1000 and 1400 $cm^{-1.}$ The broad band at about 1575 cm^{-1} is assigned to the asymmetric NO_2 stretch. There is an increase in the complexity and number of peaks in the Raman spectrum of the α RDX phase. The broad Raman peaks in the asymmetric N-O stretching regions are split into three peaks at 1594.6, 1572.7 and 1554.9 cm^{-1}. The structure of the Raman spectrum between 1000 and 1500 cm^{-1} is significantly altered. The methylene deformation bands between 1400 and 1500 cm^{-1} are split into a number of broad bands with shoulders at 1348, 1372, 1385, 1423, 1434 and 1460 cm^{-1}. The N-N stretching frequency at 1227 cm^{-1} is one of the strongest peaks between 1000 and 1500 cm^{-1} in the Raman spectrum of α RDX, while it is just a small shoulder in the β RDX Raman spectra.

The ring breathing mode in α RDX appears at 884 cm^{-1}, about 7 cm^{-1} higher than in the β RDX phase. The ring breathing mode frequency has traditionally been taken as indication of ring strain. For cyclopropane and cyclobutane, the ring breathing frequency is centered at 1188 and 1005 cm^{-1}, respectively. It is located at about 888 cm^{-1} in cyclopentane and at 801 cm^{-1} in cyclohexane. For β RDX, we found that the ring breathing frequency is about 76 cm^{-1} higher than in the chair form of cyclohexane. The evidence for ring strain suggests that intramolecular or intermolecular interactions may be important in the properties of β RDX. Assuming that the β RDX molecules have the structure shown on scheme I, we estimate the distance

among the axially positioned NO_2 groups to be about 3.9 A. This distance may be too large to allow NO_2-NO_2 repulsions to introduce the observed ring strain. Repulsions between the ring nitrogen lone electron pair and the neighboring axial hydrogen atoms, which are predicted by the calculations to be only about 2.09 A apart, may account for the observed ring strain. In this context, we expect the ring strain to decrease with the number of C-N-C units in the ring. In the eight-member ring system, HMX, that has four N-NO_2 groups, the ring breathing frequency is below 850 cm^{-1} in all the phases examined, indicating a lower ring strain than in RDX. In passing we note that the triazine ring in the α phase shows a higher strain than in the β RDX phase.

Similar differences in the Raman spectra of β and α RDX are observed in the C-H stretching region, between 2850 and 3150 cm^{-1}, shown in the right panel in figure 2. The Raman peaks observed in this region are split in two regions due to the fact that the splitting observed in the equatorial C-H stretching frequency is more pronounced, with peaks at 3073 and 3064 cm^{-1} clearly identifiable. Raman frequencies in this region are split into high and low frequency modes due to equatorial and axial stretching modes, respectively. In β RDX, these modes are observed at 2982, 2989, 3068 and 3077 cm^{-1}. The equatorial C-H stretching modes are split into peaks at 3063 and 3074 cm^{-1} in the Raman spectrum of α RDX. The Raman peaks due to the axial C-H stretching modes split into peaks at 3000.5, 2947.8 and 2906.1 cm^{-1} in α RDX.

The increase in the number of Raman signals in going from β to α RDX has traditionally being discussed in terms of a decrease in symmetry from C_{3v} to C_s. The decrease in symmetry from C_{3v} to C_s is consistent with the appearance of doublets of the $A^{/}$ and $A^{//}$ type in C_s symmetry[3]. The ring-breathing mode, for instance, that appears as a single band in the spectrum of the β phase at 877 cm^{-1} is split into a doublet at 849 and 884 cm^{-1} in the spectrum of the α phase. Further support for this model is also observed in the methylene-stretching region. The symmetric methylene C-H bond stretching band observed at about 2989 cm^{-1} in the spectrum of β RDX is split into a doublet at 2948 and 3001 cm^{-1} in the spectrum of α RDX.

The theoretical Raman spectrum for the RDX gas phase calculated at the DFT/6-311**G++ level is shown on figure 3. The optimized structure is shown on Scheme I. The agreement between observed and calculated frequencies is remarkable. The highest frequency in the calculated spectrum, due to the asymmetric stretching mode of equatorials C-H, is centered at 3193 cm^{-1}. The strongest peak in the calculated spectrum, due to the symmetric mode asymmetric NO stretch is predicted to split into peaks at 1658, 1657 and 1627 cm^{-1}. The frequency of the ring-breathing mode is predicted to appear at 936 cm^{-1} . The vibrational spectra of β and gas phase RDX have been proposed to be similar due to similarities in the structure of RDX molecules in both phases. Indeed, the infrared spectra of these phases has been measured and are remarkably similar in intensity and frequency, as predicted by theoretical DFT calculations at the B3LYP/6-311*G++ level. The calculated frequencies for gas phase RDX at the B3LYP/6-311**G++ level are in close agreement with the measured Raman frequencies in β RDX. For instance, the highest frequency mode in the Raman spectrum of β RDX is observed at 3075 cm^{-1}, which is only about 4 % lower than predicted in our calculations. The asymmetric NO_2 stretch is observed at about 1575 cm^{-1}, about 6 % lower than predicted in the calculations. Finally the frequency of the ring-breathing mode is predicted and observed at 936 and 887 cm^{-1}, a difference of about 6 %.

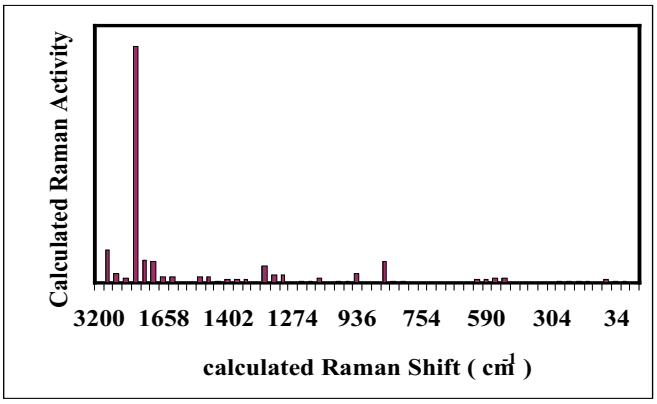

Figure 3: Calculated DFT Raman spectra of gas phase RDX at the B3LYP/6-311**G++ level. of axial C-H, is predicted at 3069 cm^{-1}.

Larger discrepancies are observed in calculated and measured Raman intensities and depolarization ratios for gas and β RDX phases, respectively. Table I summarizes calculated and measured Raman activities, depolarization ratios for the asymmetric NO_2 stretch and the ring breathing mode. Calculated values are indicated in bold, while measured values are indicated in parenthesis.

The calculations predict the symmetric stretch of axial C-H bonds to be the strongest peak in the Raman spectrum of gas phase RDX. The measurements show the symmetric ring breathing mode has the highest intensity in the Raman spectrum of β RDX. The calculations predict a depolarization ratio of 0.02 for the ring breathing frequency of gas phase RDX. Our measurements indicate that the depolarization ratio of this mode in β RDX has a value of 0.69. The measured values are free of experimental artifacts as verified in Raman measurements of the depolarization ratios of CCl_4 and even α RDX. The calculations predict 30 of the 57 normal modes in gas phase RDX to have depolarization ratios below 0.75, the value below which a mode is considered symmetric. The depolarization ratios show only eight polarized Raman bands, with

values between 0.61 and 0.74. We conclude that while the Raman frequencies predicted by theory for gas phase and measured for β RDX are similar, major differences exist among their intensities and depolarization ratios.

Mode	frequency (cm^{-1})	Raman intensity	ρ ratios
Axial C-H symmetric stretch	**3069** (2987)	**322** (2.65)	**0.12** (0.8)
Asymmetric NO_2 stretch	**1658** (1574)	**8** (1.0)	**0.75** (--)
Symmetric ring breathing mode	**936** (887)	**13** (7.50)	**0.02** (0.69)

Table I: calculated and measured Raman frequencies, activities and depolarization ratios for a few modes in gas and β RDX phases

Discussion

Raman intensities and depolarization ratios are known to be sensitive to the symmetry of a vibrational mode. For instance, molecules like CCl_4 have symmetric C-Cl stretches that have the highest intensity in the Raman spectra and depolarization ratios of 0.03. The asymmetric C-Cl stretch, on the other hand, has a depolarization ratio of 0.75. CCl_4 belong to the T_{4h} point group and is considered a molecule of high symmetry. Thus depolarization ratios are not indicative of molecular symmetry. Rather, their magnitude can be associated with the symmetry of a vibrational mode. Thus the vibrational modes in β RDX appear to have little symmetry.

Previous works have focused in the similarities between β and gas phase RDX. RDX molecules have been proposed to have a C_{3v} symmetry in the gas phase. Calculated bond lengths and angles do not reflect a C_{3v} symmetry for gas phase of RDX and predict a number of strongly polarized Raman active modes. The vapor pressure of RDX is of the order of 10^{-9} torr. Such a low vapor pressure precluded reliable measurements of the Raman spectrum and depolarization ratios for gas phase RDX. We, however, found a close agreement between calculated IR intensities and frequencies and the results of Rice and Chabalowski[3] for the RDX isomer with all the NO_2 groups in axial positions. These authors have presented a strong case to correlate the infrared spectrum of gas phase RDX and the RDX isomer with all NO_2 groups in axial position. Thus, while we are not able to measure the Raman spectrum and depolarization ratios for gas phase RDX, we believe that the structure summarized in scheme I and the results presented in table I are an adequate representation of the gas phase molecule based on the vibrational spectroscopic data available. The marked difference between the measured depolarization ratios for β RDX and calculated depolarization ratios for gas phase RDX lead us to conclude that the properties of RDX in both phases are markedly different, despite of the similarities in measured vibrational frequencies in infrared spectroscopy experiments.

Acknowledgement

We acknowledge financial support from the Federal Aviation Administration, grant number FAA 99-G-029.

References

1. Jeffrey I. Steinfeld and Jody Wornhoudt, Ann. Rev. Phys. Chem., 49, (1998), pages 203-232.

2. Richard J. Karpowicz and Thomas B. Brill, J. Phys. Chem., 88, (1984), pages 348-352.

3. Betsy M. Rice and Cary F. Chabalowiski, J. Phys. Chem. A, 101, (1997), pages 8720-8726.

4. R.L. McCreery, "Raman Spectroscopy for Chemical Analysis", Wiley and Sons, New York, N.Y., (2000).

5. Gaussian 98, Revision A.6,M. J. Frisch, G. W. Trucks, H. B. Schlegel, G. E. Scuseria, M. A. Robb, J. R. Cheeseman, V. G. Zakrzewski, J. A. Montgomery, Jr., R. E. Stratmann, J. C. Burant, S. Dapprich, J. M. Millam, A. D. Daniels, K. N. Kudin, M. C. Strain, O. Farkas, J. Tomasi, V. Barone, M. Cossi, R. Cammi, B. Mennucci, C. Pomelli, C. Adamo, S. Clifford, J. Ochterski, G. A. Petersson, P. Y. Ayala, Q. Cui, K. Morokuma, D. K. Malick, A. D. Rabuck, K. Raghavachari, J. B. Foresman, J. Cioslowski, J. V. Ortiz, B. B. Stefanov, G. Liu, A. Liashenko, P. Piskorz, I. Komaromi, R. Gomperts, R. L. Martin, D. J. Fox, T. Keith, M. A. Al-Laham, C. Y. Peng, A. Nanayakkara, C. Gonzalez, M. Challacombe, P. M. W. Gill, B. Johnson, W. Chen, M. W. Wong, J. L. Andres, C. Gonzalez, M. Head-Gordon, E. S. Replogle and J. A. Pople, Gaussian, Inc.,Pittsburgh,PA,1998.